

# Nuclear response in delta-isobar region in the ( $^3\text{He}, t$ ) reaction

V. F. Dmitriev

*Nuclear Theory Center, Indiana University, Bloomington, Indiana 47408  
and Budker Institute of Nuclear Physics, Novosibirsk 630090, Russia*

(Received 15 December 1992)

The cross section of the charge-exchange ( $^3\text{He}, t$ ) reaction in a  $\Delta$ -isobar region was calculated for a finite nucleus in terms of a relativistic nuclear response function. The medium effects modifying a  $\Delta$  and a pion propagation were considered for a finite size nucleus. The Glauber approach was used for distortion treatment of a  $^3\text{He}$  and a triton in the initial and final states. The effects determining the cross section, the peak position, and its width are discussed. A large displacement width for the  $\Delta$ -hole excitations and a considerable contribution of coherent pion production were found for the reaction on  $^{12}\text{C}$ .

PACS number(s): 25.70.Kk

## I. INTRODUCTION

The experimental studies of nuclear response in charge-exchange reactions were extended in the 1980s to high excitation energies where a first nucleon resonance, the  $\Delta$  isobar, can be excited [1]. The detailed studies were done for the ( $^3\text{He}, t$ ) charge-exchange reaction at different projectile energies [2] and different targets [3]. The properties of the  $\Delta$  excited in a nucleus were found different compared to the case of the reaction on a single nucleon. The difference was in both the peak position and the width of the resonance excited in a complex nucleus. The review of the observed phenomena can be found in a recent paper [4].

The appealing explanation of this phenomenon is related to medium effects, namely, the excitation of a pionic nuclear mode [5–9] although other effects can contribute to the high-energy part of the triton spectrum as well [10]. In this picture the  $\Delta$  in nuclear matter does not exist as separate resonance but forms a collective excitation consisted of pionic,  $\Delta$ , and nucleon degrees of freedom. In application to the ( $^3\text{He}, t$ ) reaction an extensive study of this picture was performed in [8, 9] where different approaches to distortion effects and to a calculation of the response function were used. Here we continue this line making further improvements in the distortion treatment and in the model for nuclear response.

A proper account of distortion in initial and final channels is extremely important for estimating the medium effects. An inelastic matrix element is proportional to the product of the distortion factor and transition density. It determines the average density “seen” by a projectile and it is very sensitive to a profile of the distortion factor. It was directly shown in [11] that the extreme surface reaction does not reveal any medium effects.

A theory of distortion in one-step inelastic reactions at intermediate ion energy was proposed in [12]. For inelastic reactions one should use an absorption factor different from the factor used for elastic scattering providing for both the medium effects and the magnitude of inelastic cross section. The Glauber-type approach to

the distortion treatment has no free parameters. It puts more restrictions on the elementary reaction amplitude and nuclear response function.

The surface character of the reaction advocates using the shell-model response function that describes adequately a nuclear surface. In shell-model calculations of the response function a full account of the continuum for the  $\Delta$ -hole intermediate states is necessary since the  $\Delta$ -hole multipoles at least up to  $L = 10$  must be retained to get saturation at the high-energy wing of the peak in the reaction on  $^{12}\text{C}$ . As will be shown below, in a finite nucleus, due to a different magnitude of the medium effects for different  $\Delta$ -hole multipoles, there is an additional displacement shift so part of the observed width can be attributed to this displacement. Besides, on a finite nucleus the process of coherent pion production is possible. The process is absent in infinite nuclear matter and it contributes to the shift of the peak position as well.

In the present calculation we use a relativistic  $\Delta$ -hole response function. As was shown in [6] the relativistic expression for the response function in nuclear matter differs from its nonrelativistic analog. The difference comes from two sources. First, from the proper relativistic kinematics allowing one to reproduce more accurately the position of the  $\Delta$  peak in  $^1\text{H}(p, n)\Delta^{++}$  and  $^1\text{H}(^3\text{He}, t)\Delta^{++}$  reactions [13]. Second, from the proper treatment of spin- $\frac{3}{2}$  variables of a moving  $\Delta$ . The higher powers of momentum in the relativistic  $\Delta$  propagator produce nonresonant terms in the  $\Delta$ -hole loop and a kinematical factor at the resonant term that quenches it for about 20% compared to its nonrelativistic expression [6]. Both these factors together with nonresonant  $\pi N$  partial waves decrease attraction in the spin-longitudinal channel and shift the pionic mode in nuclear matter to higher energy, thus advocating for a lower value of short-range interaction constant  $g'_\Delta$  [7].

In the next section we discuss the motivation for choosing the one-pion-exchange (OPE) model for the reaction amplitude that is a driving force for the nuclear response. In Sec. IV the pionic response function of a finite nucleus

is discussed. The distortion effects and the cross-section calculation are discussed in Sec. V. In Sec. VI we describe the features of the triton spectrum.

## II. REACTION AMPLITUDE

Let us discuss briefly the models for the elementary charge-exchange reaction  ${}^1\text{H}(p, n)\Delta^{++}$ . From the early 1960s it was shown this reaction can be described by the OPE model [14], at least at low momentum transfer. This analysis has been extended for a wide range of the proton energies in [15], and has been repeated with some minor modifications in connection with the analysis of the  ${}^1\text{H}({}^3\text{He}, t)\Delta^{++}$  reaction in [13]. It was shown that all existing data in the region of low momentum transfer are well described by OPE with the soft monopole  $\pi NN$  and  $\pi N\Delta$  form factors

$$F(q^2) = \frac{\Lambda^2 - \mu^2}{\Lambda^2 - q^2}. \quad (1)$$

The parameter  $\Lambda = 650$  MeV at low proton energy and slightly decreases with the proton energy reflecting an increase of the absorption effects at high energy. With these soft form factors (1) the main contribution to the  $\Delta$  production comes from the direct graph shown in Fig. 1. The exchange contribution with the soft form factors (1) is small.

The OPE amplitude is completely longitudinal with respect to the momentum transfer. In the other model used for the description of the  $\Delta$  production at 800 MeV proton energy [16] the transverse part of the amplitude was described by  $\rho$  exchange and hard form factors with  $\Lambda = 1.2$  GeV and  $\Lambda = 1.7$  GeV were used for  $\pi N\Delta$  and  $\rho N\Delta$  vertexes. The magnitude of the cross section and the momentum transfer dependence are reproduced in this model due to cancellation between the direct and exchange parts of the amplitude. The cancellation is rather delicate and at higher proton energy it can be broken resulting in the wrong momentum transfer dependence of the cross section [13].

The spin structure of the pion production amplitude in proton-proton collisions was studied in experiment with polarized beam in the range of beam momentum from 1.18 GeV/c to 12 GeV/c [17, 18]. The remarkable feature of the measured spin density matrix elements is their weak dependence on the beam momentum in all the momentum range. This feature is inherent to the exchange of the spin-0 boson. Pure one-pion exchange certainly does not reproduce the spin density matrix. But, as the authors pointed out, the same pion exchange corrected for the absorption of a projectile fits well all the data at low four-momentum transfer  $|t|$ .

At very high energy the situation is different. The  $\pi$ -exchange contribution decreases as  $s^{-2}$ , where  $s$  is the center-of-mass energy squared, while for the  $\rho$  exchange

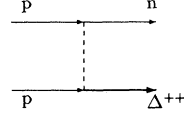


FIG. 1. Direct OPE graph for the  $\Delta$  production.

the decrease is slower. Its contribution falls down like  $s^{-2+\alpha(0)}$  for small momentum transfer where  $\alpha(t)$  is the corresponding Regge trajectory. Thus, in the asymptotic region at high energy one should expect the dominance of the  $\rho$  exchange even at forward angles. Below 20 GeV the cross section for forward scattering follows the  $1/s^2$  law [19] so, the contribution of  $\rho$  exchange at intermediate energies is believed to be small.

For the  ${}^1\text{H}({}^3\text{He}, t)\Delta^{++}$  reaction the situation is similar to the  $(p, n)$  case. The  $\pi$  exchange with the soft form factors (1) gives a reasonable description of the absolute cross section and the tritium spectrum at a forward angle for all existing data [13]. Nevertheless, at the kinetic energy of  ${}^3\text{He}$  2 GeV, which is close in kinematics to 800 MeV  $(p, n)$  one can get a good description using  $\pi + \rho$  exchanges as well [20]. It would be very desirable to extend the last analysis to higher  ${}^3\text{He}$  energies.

Referring to the results of the absolute cross-section calculations for the  ${}^1\text{H}({}^3\text{He}, t)\Delta^{++}$  reaction [13] we choose for our study the OPE amplitude of the elementary reaction. In that way we stress our attention on the response function of a finite size nucleus and the modifications of the elementary amplitude due to various medium effects in the pionic mode channel.

It should be pointed out that the choice of spin-longitudinal elementary amplitudes does not imply the full nuclear amplitudes to be spin longitudinal. The absorption changes the spin structure of the amplitude. A study of this effect and calculation of spin observables will be presented separately.

## III. NUCLEAR MATTER RESPONSE TO THE PIONIC PROBE

### A. $({}^3\text{He}, t)$ cross section in plane wave approximation

It is convenient to start with the plane waves for both projectile and ejectile in order to obtain an expression for the cross section that can be easily generalized to the distorted waves. In the plane wave impulse approximation (PWIA) the cross section is proportional to the matrix element, shown in Fig. 1, squared and summed over final nuclear and  $\Delta$  states:

$$T = \int d^3r \Gamma_{\pi\text{Het}}(\mathbf{r}) G_0(\mathbf{r} - \mathbf{r}') \cdot \Gamma_{\pi N\Delta}(\mathbf{r}') d^3r'. \quad (2)$$

For plane waves  $\Gamma \sim \exp(i\mathbf{q} \cdot \mathbf{r})$ , it gives for the cross section

$$\frac{d^2\sigma}{dE'd\Omega} = \frac{M_{\text{He}}^2}{4\pi^2} \frac{p'}{p} |\Gamma_{\pi\text{Het}}(\mathbf{q})|^2 \sum_{\Delta h} \delta(\omega - E_{\Delta h}) n_h |\Gamma_{\pi N\Delta}(\mathbf{q})|^2 |G_0(q)|^2. \quad (3)$$

The expression under the sum is just an imaginary part of the pionic self-energy in nuclear medium:

$$\text{Im}\Pi_{\Delta}(\omega, \mathbf{q}, \mathbf{q}) = \pi \sum_{\Delta h} \delta(\omega - E_{\Delta h}) |\Gamma_{\pi N \Delta}|^2 n_h. \quad (4)$$

Using the pionic self-energy (4) we obtain the final expression for the cross section suitable for inclusion of medium effects:

$$\frac{d^2\sigma}{dE'd\Omega} = \frac{M_{\text{He}}^2}{4\pi^3} \frac{p'}{p} |\Gamma_{\pi \text{Het}}(\mathbf{q})|^2 G_0^*(q) \text{Im}\Pi_{\Delta}(\omega, \mathbf{q}, \mathbf{q}) G_0(q). \quad (5)$$

### B. Medium effects in nuclear matter

The main effect of the nuclear medium is the renormalization of the pion propagator by intermediate  $\Delta$ -hole loops giving the major contribution to the pionic self-energy (4) near the  $\Delta$  resonance. To take it into account one must change in (5) the bare pion propagator  $G_0(q)$  for the dressed one  $G(\omega, \mathbf{q})$ , where

$$G(\omega, \mathbf{q}) = \frac{1}{q^2 - \mu^2 - \Pi_{\Delta}(\omega, \mathbf{q})}.$$

Making this change we are going out of the scope of the impulse approximation.

The imaginary part of the bare pion propagator is equal to zero for negative  $q^2$ . Using it we obtain  $G^*(\omega, \mathbf{q}) \text{Im}\Pi_{\Delta}(\omega, \mathbf{q}) G(\omega, \mathbf{q}) = -\text{Im}G(\omega, \mathbf{q})$ . With these changes the cross section (5) becomes

$$\frac{d^2\sigma}{dE'd\Omega} = -\frac{M_{\text{He}}^2}{4\pi^3} \frac{p'}{p} |\Gamma_{\pi \text{Het}}(\mathbf{q})|^2 \text{Im}G(\omega, \mathbf{q}). \quad (6)$$

It is clear from (6) the pion propagator  $G(\omega, \mathbf{q})$  in the nuclear medium is just the response function to a virtual pion probe. The excitation created by a virtual pion is no more a pure  $\Delta$  hole but a superposition of the  $\Delta$  hole and pionic degrees of freedom usually called the pionic mode.

The unquenched nonrelativistic  $\Delta$ -hole self-energy (4) produces too much of an attraction giving unreasonably low excitation energy for the pionic mode. In order to make the description more accurate several effects should be taken into account. First, we used relativistic expression for the resonant  $\Delta$ -hole loop that was found in [6]. The relativistic corrections produce some nonresonant terms, therefore more accurate  $\pi N$ -scattering amplitudes reproducing nonresonant  $s_{\frac{1}{2}}$  and  $p_{\frac{1}{2}}$  partial waves should be used. For this purpose one should add Born diagrams with a nucleon intermediate state, a  $u$ -channel  $\Delta$  diagram, and a  $\sigma$  term arising from the  $\sigma$  commutator [21]. Second, the short-range  $N\Delta$  correlations must be taken into account:

$$W(\mathbf{r}_1, \mathbf{r}_2) = \frac{f_{\Delta}^2}{\mu^2} g'_{\Delta} (\mathbf{S}_1^{\dagger} \cdot \mathbf{S}_2) (\mathbf{T}_1^{\dagger} \cdot \mathbf{T}_2) \delta(\mathbf{r}_1 - \mathbf{r}_2). \quad (7)$$

In nuclear matter the effect of short-range correlations can be accounted in the following way. Let us define

according to [6] the  $\Delta$ -hole response function  $\chi(\omega, \mathbf{q})$  by

$$\begin{aligned} \Pi_{\Delta}(\omega, \mathbf{q}) = & \left( \frac{\Lambda^2 - \mu^2}{\Lambda^2 - q^2} \right)^2 \mathbf{q}^2 \frac{(m + m_{\Delta})^2 - q^2}{4m_{\Delta}^2} \chi(\omega, \mathbf{q}) \\ & + \frac{2}{9} \left( \frac{f_{\Delta}(q^2)}{\mu} \right)^2 \frac{m}{m_{\Delta}^2} n \mathbf{q}^2 \\ & + \frac{4}{9} \left( \frac{f_{\Delta}(q^2)}{\mu} \right)^2 \frac{1}{m_{\Delta}} \left( 1 + \frac{m}{m_{\Delta}} \right) n q^2, \end{aligned} \quad (8)$$

where  $n$  is the nuclear density (in [6]  $n$  was in fact the proton density) and  $f_{\Delta}(q^2)$  is the  $\pi N \Delta$  coupling constant with the form factor (1). The  $\Delta$ -hole self-energy corrected for the short-range interaction (7) can be written as

$$\begin{aligned} \tilde{\Pi}_{\Delta}(\omega, \mathbf{q}) = & \left( \frac{\Lambda^2 - \mu^2}{\Lambda^2 - q^2} \right)^2 \mathbf{q}^2 \frac{(m + m_{\Delta})^2 - q^2}{4m_{\Delta}^2} \tilde{\chi}(\omega, \mathbf{q}) \\ & + \frac{2}{9} \left( \frac{f_{\Delta}(q^2)}{\mu} \right)^2 \frac{m}{m_{\Delta}^2} n \mathbf{q}^2 \\ & + \frac{4}{9} \left( \frac{f_{\Delta}(q^2)}{\mu} \right)^2 \frac{1}{m_{\Delta}} \left( 1 + \frac{m}{m_{\Delta}} \right) n q^2, \end{aligned} \quad (9)$$

where

$$\tilde{\chi}(\omega, \mathbf{q}) = \frac{\chi(\omega, \mathbf{q})}{1 - g'_{\Delta} \chi(\omega, \mathbf{q})}. \quad (10)$$

A similar effect should be taken into account for the nucleon-hole response function as well. But, in the region of interest in excitation energy its contribution is negligible and will be omitted below. In contrast, the backward  $\Delta$ -hole loops and the  $\sigma$  term must be retained since they have their own dependence on the virtual pion mass  $q^2$  that influences the position of the pionic branch in nuclear matter.

Finally, the virtual pion can be absorbed in a nuclear medium emitting two or more nucleons. In the resonance region the absorption goes via intermediate  $\Delta$  and it can be described by a  $\Delta$ -nucleus optical potential. At lower energies the other mechanisms with different intermediate states contribute to the absorption. To take it into account the Ericson-Ericson-type optical potential proposed first for pionic atoms [22] can be used

$$V_{2N} = -4\pi i \text{Im}C n^2(r) \mathbf{q}^2,$$

where  $n(r)$  is the nuclear matter density. For pionic atoms  $\text{Im}C = 0.08 \left( \frac{\hbar}{\mu c} \right)^6$ . It was obtained from the fit of the mesoatomic level width and contains all absorption mechanisms including the intermediate  $\Delta$ . Using this value in our case will give double counting since intermediate  $\Delta$  is considered explicitly. Thus,  $\text{Im}C$  should be considered as a free parameter accounting another absorption mechanisms. We found, however, that the triton spectrum is almost insensitive to  $\text{Im}C$  in the range  $\text{Im}C = 0-0.08$ . For this reason we did not study carefully this possibility of keeping  $\text{Im}C = 0$ .

With these corrections the pion self-energy in nuclear matter is

$$\Pi(\omega, \mathbf{q}) = \tilde{\Pi}_\Delta(\omega, \mathbf{q}) + \frac{1}{f_\pi^2} \left( 1 - \frac{2q^2}{\mu^2} \right) \sigma(0)n(r) + V_{2N}, \quad (11)$$

where  $f_\pi$  is the pion decay constant  $f_\pi = 133$  MeV and  $\sigma(0)$  is the  $\sigma$  commutator for forward pion scattering.  $\tilde{\Pi}_\Delta(\omega, \mathbf{q})$  includes both forward and backward  $\Delta$ -hole loops corrected for short-range correlations.

#### IV. RESPONSE FUNCTION OF A FINITE NUCLEUS

For a finite nucleus it is convenient to work in the configuration space where the self-energy (11) and the pion propagator become the functions of two distinct variables instead of functions of the distance between coordinate points in nuclear matter:

$$\Pi(\omega, \mathbf{r} - \mathbf{r}') \rightarrow \Pi(\omega, \mathbf{r}, \mathbf{r}').$$

The  $\pi N\Delta$  vertex in the configuration space is

$$\Gamma_{\pi N\Delta}(\mathbf{r}, \mathbf{r}') = -i\mathbf{T}(\mathbf{S} \cdot \nabla) \frac{f_\Delta}{\mu} \frac{\Lambda^2 - \mu^2}{4\pi} \frac{\exp(-\kappa|\mathbf{r} - \mathbf{r}'|)}{|\mathbf{r} - \mathbf{r}'|}, \quad (12)$$

where  $\kappa^2 = \Lambda^2 - \omega^2$ .

For a spherical nucleus the self-energy (11) has a simple multipole expansion:

$$\Pi(\omega, \mathbf{r}, \mathbf{r}') = \sum_{JM} \Pi_J(r, r') Y_{JM}^*(\mathbf{n}) Y_{JM}(\mathbf{n}').$$

A similar expansion exists for the  $\pi N\Delta$  vertex

$$\Gamma_{\pi N\Delta}(\mathbf{r} - \mathbf{r}') = \sum_{JLM} \Gamma_{JL}^0(r, r') Y_{JM}^*(\mathbf{n}) T_{JM}^L(\mathbf{n}'), \quad (13)$$

where the tensor operator

$$T_{JM}^L(\mathbf{n}') = \mathbf{S} \cdot \mathbf{Y}_{JM}^L(\mathbf{n}) = [\mathbf{S} \wedge Y_{Lm}(\mathbf{n})]_{JM}, \quad (14)$$

and the radial vertex  $\Gamma_{JL}^0(r, r')$  is

$$\Gamma_{JL}^0(r, r') = i(L - J) \frac{f_\Delta}{\mu} \frac{2\kappa^2(\Lambda^2 - \mu^2)}{\pi} \sqrt{\frac{J + L + 1}{2(2J + 1)}} \times \begin{cases} i_L(\kappa r) k_J(\kappa r') & \text{if } r < r', \\ -i_J(\kappa r') k_L(\kappa r) & \text{if } r > r', \end{cases} \quad (15)$$

here  $i_L(x)$  and  $k_L(x)$  are the spherical Bessel functions with an imaginary argument. This is the advantage of using the simple scalar form (1).

The  $\Delta$ -hole response function  $\chi$  can be expanded using the set of tensor operators (14)

$$\begin{aligned} \chi_{LL'}^J(r, r') &= \frac{1}{2J + 1} \sum_{j_N l_N l_\Delta} \langle j_N l_N \| T_J^L \| j_\Delta l_\Delta \rangle \\ &\times \langle j_\Delta l_\Delta \| T_J^{L'} \| j_N l_N \rangle \frac{m}{m_\Delta} [g_{j_\Delta l_\Delta}(E(\omega) + i\Gamma(\omega)/2; r, r') + g_{j_\Delta l_\Delta}(E(-\omega); r, r')] \\ &\times n_{j_N l_N} R_{j_N l_N}(r) R_{j_N l_N}(r'), \end{aligned} \quad (16)$$

where  $n_{j_N l_N}$  are the nucleon occupation numbers,  $R_{j_N l_N}(r)$  is the radial wave function of bounded nucleon.  $g_{j_\Delta l_\Delta}(E; r, r')$  is the Green's function of the radial Schrödinger equation for  $\Delta$  moving in the mean nuclear optical potential. The energy parameter  $E(\omega) = \frac{m}{m_\Delta}(\omega + \frac{\omega^2}{2m} + \epsilon_{j_N l_N} - \frac{m_\Delta^2 - m^2}{2m})$ , where  $\epsilon_{j_N l_N}$  is the energy of a bounded nucleon, takes into account relativistic correction for kinematics at high  $\omega$ . The Green's function was calculated using two independent solutions of the radial Schrödinger equation.

The resonance part of the  $\Delta$ -hole contribution to the pion self-energy was calculated using the following expression:

$$\begin{aligned} \tilde{\Pi}_R^J(\omega; r, r') &= \sum_{LL'} \int \rho^2 d\rho \rho'^2 d\rho' \Gamma_{JL}^0(r, \rho) \chi_{LL'}^J(\rho, \rho') \\ &\times \Gamma_{JL'}^*(\rho, r'), \end{aligned} \quad (17)$$

where  $\Gamma_{JL}$  related to  $\Gamma_{JL}^0$  via the linear integral equation accounting the short-range correlations (7):

$$\Gamma_{JL}(r, \rho)$$

$$\begin{aligned} &= \Gamma_{JL}^0(r, \rho) + g' \left( \frac{f_\Delta}{\mu} \right)^2 \\ &\times \sum_{L'} \int \rho'^2 d\rho' \Gamma_{JL'}(r, \rho') \chi_{LL'}^J(\rho', \rho). \end{aligned} \quad (18)$$

#### V. THE EFFECTS OF DISTORTION

For numerical calculations it is convenient to come back from expression (6) to a more complex one similar to (5):

$$\frac{d^2\sigma}{dE'd\Omega} = \frac{M_{\text{He}}^2}{4\pi^2} \frac{p'}{p} \overline{\Gamma_{\pi\text{Het}}^\dagger G^* \text{Im} \Pi G \Gamma_{\pi\text{Het}}}. \quad (19)$$

The product sign means integration over all coordinates in the configuration space and the overbar is the averaging and summing over spins of a  ${}^3\text{He}$  and a triton.

In infinite matter the  $\Delta$ -hole contribution (19) would

be the only one in the inclusive cross section. In a finite nucleus, however, the cut of a bare pionic line gives a nonzero contribution corresponding to coherent pion production:

$$\frac{d^2\sigma_c}{dE'd\Omega} = -\frac{M_{\text{He}}^2}{4\pi^2} \frac{p'}{p} \Gamma_{\pi\text{Het}}^\dagger G^* \Pi^* \text{Im} G_0 \Pi G \Gamma_{\pi\text{Het}}. \quad (20)$$

In the plane wave approximation the  $\pi^3\text{Het}$  vertex is

$$\Gamma_{\pi\text{Het}}(\mathbf{r}) = \sqrt{2}(\boldsymbol{\sigma} \cdot \tilde{\mathbf{q}}) F(q^2) \frac{f_N(q^2)}{\mu} \exp(i\mathbf{q} \cdot \mathbf{r}), \quad (21)$$

where the effective momentum transfer  $\tilde{\mathbf{q}}$  in laboratory system in first order of  $\frac{\omega}{E+M}$  is

$$\tilde{\mathbf{q}} = \mathbf{q} - \frac{1}{2} \frac{\omega}{E+M} (\mathbf{p} + \mathbf{p}').$$

$M$  is the  $^3\text{He}$  mass and  $E$  is its total energy. The effective momentum transfer squared coincides with the four-momentum transfer squared.  $F(q^2)$  is the ( $^3\text{He}, t$ ) transition form factor.

The multipole expansion of the vertex looks as follows:

$$\begin{aligned} \exp[-\tfrac{1}{2}\chi_{\text{in}}(\mathbf{r}_\perp, \mathbf{q})] &= \left(1 - \frac{1}{A} \bar{\gamma} T(\mathbf{r}_\perp)\right)^{A-1} \\ &\times \int d^3s_1 d^3s_2 d^3s_3 \exp(i\mathbf{q} \cdot \mathbf{s}_1) \Psi^*(\mathbf{s}_1, \mathbf{s}_2, \mathbf{s}_3) \\ &\times \left(1 - \frac{1}{A} \bar{\gamma} T(\mathbf{r}_\perp + \mathbf{s}_{2\perp} - \mathbf{s}_{1\perp})\right)^A \left(1 - \frac{1}{A} \bar{\gamma} T(\mathbf{r}_\perp + \mathbf{s}_{3\perp} - \mathbf{s}_{1\perp})\right)^A \\ &\times \Psi(\mathbf{s}_1, \mathbf{s}_2, \mathbf{s}_3) \delta(\mathbf{s}_1 + \mathbf{s}_2 + \mathbf{s}_3), \end{aligned} \quad (26)$$

where  $T(\mathbf{r}_\perp)$  is the thickness function

$$T(\mathbf{r}_\perp) = \int_{-\infty}^{\infty} \rho(\mathbf{r}_\perp, z) dz,$$

and  $\rho(\mathbf{r}_\perp, z)$  is the target density. The

$$\bar{\gamma} = -i \frac{2\pi}{p_{\text{lab}}} f(0)$$

is related to the elastic nucleon-nucleon scattering amplitude at a given energy per nucleon and  $\Psi(\mathbf{s}_1, \mathbf{s}_2, \mathbf{s}_3)$  is the wave function of  $^3\text{He}$  or the triton depending on the internal coordinates  $\mathbf{s}$ . The value of  $\bar{\gamma}$  used in calculations is  $\bar{\gamma} = (2.1 - i0.26) \text{ fm}^2$ . It was found from the fit of elastic proton nucleus scattering [23].

Two important features of the distortion factor (26) should be mentioned. First, the ( $^3\text{He}, t$ ) form factor can not be in general separated from the effects of distortion. In a particular case only, for  $0^\circ$  scattering angle, and for oscillator wave functions of  $^3\text{He}$  and a triton, the form factor can still be factorized. Second, since the vertex (25) has a gradient coupling and the distortion factor (26) depends on the transversal coordinates, some transversal components arise in the reaction amplitude even if it was before the pure longitudinal one.

$$\Gamma_{\pi\text{Het}}(\mathbf{r}) = \sum_{JLM} \Gamma_{LJM}^N(r) t_{JM}^L(\mathbf{n}), \quad (22)$$

where  $t_{JM}^L(\mathbf{n})$  are the tensor operators analogous to (14):

$$t_{JM}^L(\mathbf{n}) = \boldsymbol{\sigma} \cdot \mathbf{Y}_{JM}^L(\mathbf{n}) = [\boldsymbol{\sigma} \wedge Y_{LM}]_{JM}. \quad (23)$$

For plane waves the radial vertex is

$$\begin{aligned} \Gamma_{LJM}^{0N}(r) &= \sqrt{2} i^L j_L(qr) [\tilde{\mathbf{q}} \wedge Y_{Lm}^*(\hat{\mathbf{q}})]_{JM} \\ &\times \frac{f_N(q^2)}{\mu} F(q^2). \end{aligned} \quad (24)$$

The distortion of the incoming and outgoing waves has been taken into account via an inelastic distortion factor [12]. With this factor the  $\pi^3\text{Het}$  vertex becomes

$$\begin{aligned} \Gamma_{\pi\text{Het}}(\mathbf{r}) &= \sqrt{2} \left( -i(\boldsymbol{\sigma} \cdot \nabla) - \frac{1}{2} \frac{\omega}{E+M} [\boldsymbol{\sigma} \cdot (\mathbf{p} + \mathbf{p}')] \right) \\ &\times \frac{f_N(q^2)}{\mu} \exp(i\mathbf{q} \cdot \mathbf{r}) \exp[-\tfrac{1}{2}\chi_{\text{in}}(\mathbf{r}_\perp, \mathbf{q})]. \end{aligned} \quad (25)$$

The distortion factor  $\exp[-\tfrac{1}{2}\chi_{\text{in}}(\mathbf{r}_\perp, \mathbf{q})]$  is [12]

The multipole expansion of the distorted vertex (25) can be obtained directly by multiplying it on  $t_{JM}^L(\mathbf{n})$ , taking trace over spin variables, and integrating over angles of the unit radius vector  $\mathbf{n}$ :

$$\Gamma_{LJM}^N(r) = \frac{1}{2} \text{Tr} \int d\mathbf{n} \left( t_{JM}^L(\mathbf{n}) \Gamma_{\pi\text{Het}}(\mathbf{r}) \right). \quad (27)$$

The separate multipoles contribute independently into cross section (19), that becomes

$$\frac{d^2\sigma}{dE'd\Omega} = \frac{M_{\text{He}}^2}{4\pi^3} \frac{p'}{p} \sum_{LJM} \Gamma_{LJM}^{*N} G_L^* \text{Im} \Pi_L G_L \Gamma_{LJM}^N. \quad (28)$$

A similar expansion exists for the coherent pion contribution (20).

For a numerical calculation it is convenient to define the function

$$w_{LJM}(r) = \int_0^\infty r'^2 dr' G_L(r, r') \Gamma_{LJM}^N(r'),$$

that is the pion field at the reaction point generated by the source  $\Gamma_{LJM}^N(r')$ . The integration over  $r'$  is not well defined numerically since the integrand is an oscillating function not decreasing at infinity. An implicit integra-

tion can be done in the following way. The function  $w_{LJM}(r)$  satisfies the integro-differential equation

$$\int_0^\infty r'^2 dr' G_L^{-1}(r, r') w_{LJM}(r') = \Gamma_{LJM}^N(r), \quad (29)$$

$$\frac{d^2\sigma}{dE'd\Omega} = \frac{M_{He}^2}{4\pi^3} \frac{p'}{p} \sum_{LJM} w_{LJM}^* (\text{Im}\Pi_L - \Pi_L^* \text{Im}G^0 \Pi_L) w_{LJM}. \quad (30)$$

In expression (30) the integration over coordinates goes effectively in a finite range, inside the target nucleus.

## VI. THE TRITON SPECTRA FOR $^{12}\text{C}({}^3\text{He}, t)$ REACTION AT 2 GeV

### A. Parameters of the single-particle potentials

The nucleon single-particle potential used for the wave functions of the bound nucleons has been taken in the standard Woods-Saxon form:

$$U(r) = V_0 f(r) + V_{LS} \frac{\lambda_\pi^2}{r} \frac{df(r)}{dr} (\boldsymbol{\sigma} \cdot \mathbf{l}) + V_C(r),$$

where  $f(r) = \frac{1}{1 + \exp(\frac{r-R}{a})}$ ,  $\lambda_\pi$  is the pion Compton wavelength, and  $V_C(r)$  is the Coulomb potential for protons that was taken as the potential of a uniformly charged sphere. The parameters of the potential were chosen to reproduce the positions of  $p_{3/2}$  and  $p_{1/2}$  levels in  $^{12}\text{C}$ . They are listed in Table I. The response function (16) was found not very sensitive to the parameters of the nucleon potential.

The situation is, however, different for the optical  $\Delta$ -nucleus potential that has been taken in similar Woods-Saxon form:

$$U_\Delta(r) = (V_\Delta + iW_\Delta) f(r) + (V_{\Delta LS} + iW_{\Delta LS}) \frac{\lambda_\pi^2}{r} \frac{df(r)}{dr} (\mathbf{s}_\Delta \cdot \mathbf{l}) + V_{\Delta C}(r),$$

where  $s_\Delta$  are the spin-3/2 matrices. Figure 2 shows two triton spectra for the  $\Delta$ -hole contribution demonstrating sensitivity to the real part of the  $\Delta$ -nucleus optical potential. In the absence of the  $\Delta$ -nucleus interaction the peak position coincides with the one in the reaction on the free proton. The attraction produced by the real part of the potential in the final state increases the cross section and shifts the peak position on 15–20 MeV down.

This sensitivity demands independent restrictions on the magnitude of the potential. Such restrictions can be

that can be solved numerically using the condition for Feynman propagator  $G_L(r, r') = G_L^{(+)}(r, r')$  at positive energy. Since  $G_L^{(+)}(r, r')$  has an outgoing wave at infinity, it fixes the solution of Eq. (29). The cross section expressed in terms of  $w_{LJM}(r)$  is

found in the photoabsorption process where the influence of the pion-exchange interaction is negligible. The analysis performed in [24] gave for the real part of the potential  $V_\Delta = 32.5$  MeV and for the imaginary part  $W_\Delta = 45$  MeV. In both cases the potential was chosen proportional to the density. The theoretical study of the  $\Delta$ -nucleus potential in nuclear matter performed in [25] revealed the momentum dependence of the real part of the potential. It is changing from 40 to 30 MeV in the momentum range of  $\Delta$  from 100 to 400 MeV/c. A similar nonlocality was found in the imaginary part too, although the fits of it in different nuclei are not very supportive. The parameters of the optical potential used in our calculations are listed in Table II. The radius  $R$  and the diffuseness  $a$  were kept the same as for nucleons.

### B. Medium effects of pion renormalization

The main feature of the pionic self-energy near the resonance is its large imaginary part. It is instructive to study separately the effects of real and imaginary parts of the self-energy on the triton spectra. Figure 3 shows three spectra where either a real or imaginary part of the self-energy was accounted in comparison to the quasifree case. The real part of the self-energy is attractive and it brings more strength to the  $\Delta$ -hole peak just in analogy with particle-hole giant resonances. The peak position, however, does not change much. The imaginary part

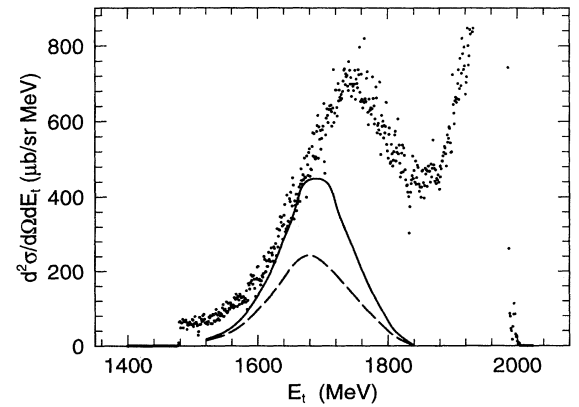


FIG. 2. Quasifree  $\Delta$  production. Dashed line, no  $\Delta$ -nucleus potential, the peak position practically coincides with the one in the reaction on a free proton. Solid line,  $V_\Delta = -35$  MeV.

TABLE I. Parameters of the single-particle nucleon potential.

	$V_0$ (MeV)	$V_{LS}$ (MeV)	$R$ (fm)	$R_{LS}$ (fm)	$a$ (fm)	$a_{LS}$ (fm)
$p$	57	12	$1.25A^{1/3}$	$1.25A^{1/3}$	0.53	0.53
$n$	57	12	$1.25A^{1/3}$	$1.25A^{1/3}$	0.53	0.53

TABLE II. Parameters of the  $\Delta$ -nucleus optical potential. The radius and diffuseness are the same as for the nucleons.

$V_\Delta$ (MeV)	$W_\Delta$ (MeV)	$V_{LS\Delta}$ (MeV)	$W_{LS\Delta}$ (MeV)
35	40	5	0

takes all this strength back decreasing the cross section due to incoherent  $\Delta$  decay thus, when both parts are taken into account, the cross section appeared close to its quasifree magnitude as it is shown in Fig. 3 and Fig. 4.

In Fig. 3 one can see that the imaginary part of the self-energy also produces some shift in the peak position. The origin of the shift is, however, different from the shift due to the real part. To understand its origin let us return to nuclear matter and compare two expressions for the cross sections with and without renormalization of the pion propagator. Without renormalization the cross section is proportional to

$$\frac{\text{Im}\Pi(\omega, \mathbf{q})}{(q^2 - \mu^2)^2},$$

while in the other case it is proportional to

$$\frac{\text{Im}\Pi(\omega, \mathbf{q})}{(q^2 - \mu^2)^2 + [\text{Im}\Pi(\omega, \mathbf{q})]^2}.$$

For simplicity the real part is omitted in this expression. The first case corresponds to a quasifree mechanism and the peak position is at the same place as in the reaction on a proton. In the second case the cross section starts to grow at the same threshold but at the resonance where  $\text{Im}\Pi(\omega, \mathbf{q}) > (q^2 - \mu^2)$  we have the cross section proportional to

$$\frac{1}{\text{Im}\Pi(\omega, \mathbf{q})}.$$

Thus, instead of a maximum, the cross section appeared

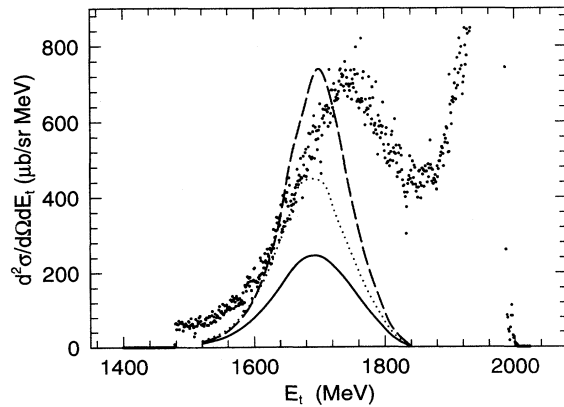


FIG. 3. Effects of real and imaginary parts of the pion self-energy on the  $\Delta$ -hole part of the triton spectrum. Dotted line, no medium effects for pion. Dashed line, effect of the real part of the self-energy. Solid line, effect of the imaginary part of the pion self-energy.

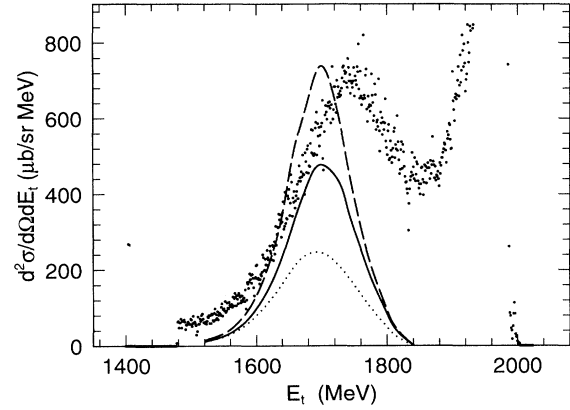


FIG. 4. Dashed line, effect of the real part. Dotted line, effect of the imaginary part. Solid line, full pion self-energy included.

to be small at this energy. Since the cross section is growing from threshold one can immediately conclude that the maximum of the cross section will be below the resonance position. Figure 5 demonstrates this effect for the  $L = 0$  multipole in the case of a finite nucleus. This effect is not so much pronounced for higher multipoles that determine the magnitude of the cross section. The higher multipoles undergo smaller medium effects since they are peaked at a nuclear surface where the density is small. Therefore, the overall shift of the peak position is smaller than for  $L = 0$ . The imaginary part of the optical  $\Delta$ -nucleus potential makes this effect stronger as is shown in Fig. 6.

### C. Contribution of separate multipoles

The contribution of separate multipoles to the triton spectrum is shown in Fig. 7. The contribution of the low multipoles  $L = 0$  and  $L = 1$  is almost negligible due to strong absorption of the incoming and outgoing ions. The main contribution comes from the multipoles between  $L = 2$  and  $L = 6$  although higher multipoles,

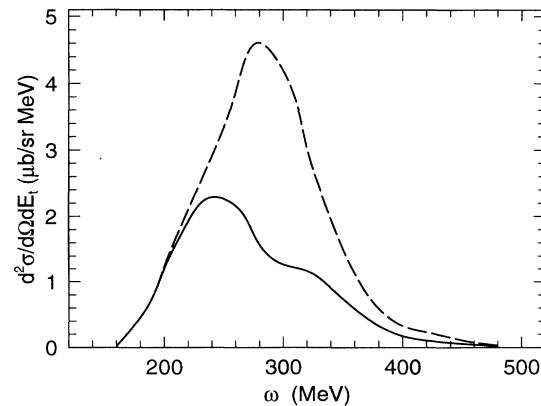


FIG. 5. The shift of the peak position due to the imaginary part of the pion self-energy for the  $L = 0$   $\Delta$ -hole multipole.

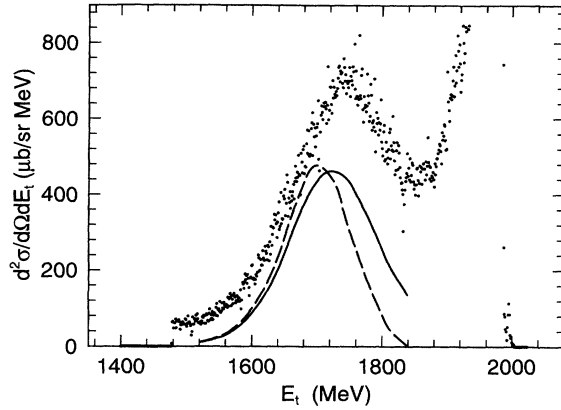


FIG. 6. Influence of the imaginary part of the  $\Delta$ -nucleus optical potential. Dashed line  $W_\Delta = 0$ . Solid line  $W_\Delta = 40$  MeV.

at least up to  $L = 10$ , have to be considered at higher excitation energy.

It should be pointed out that strong  $L$  dependence of the absorption at low multipoles will result in an additional change of the spin structure of the full reaction amplitude. Pure  $(\sigma \cdot \mathbf{q})$  correlation produces a definite relation between the  $L - 1$  and  $L + 1$  components of the  ${}^3\text{He}$ - $t$  vertex. Different absorption for different multipoles destroys this relation, thus creating a new spin structure of the vertex. This effect is in addition to the one mentioned in Sec. V and it exists for all spin-dependent amplitudes.

Another feature clearly seen in Fig. 7 is rather wide, spreading of the different multipole contributions. The  $L = 2$  contribution is most sensitive to the medium effects shifting down the transition strength. It has the largest downward shift in the peak position. The absorption of  ${}^3\text{He}$  and  $t$  is smaller for  $L = 2$  compared to  $L = 0$  resulting in a sizable contribution to the cross section. Higher multipoles have smaller medium effects and their peak positions are at more and more higher excitation energies. This produces a large displacement width of summed triton spectrum.

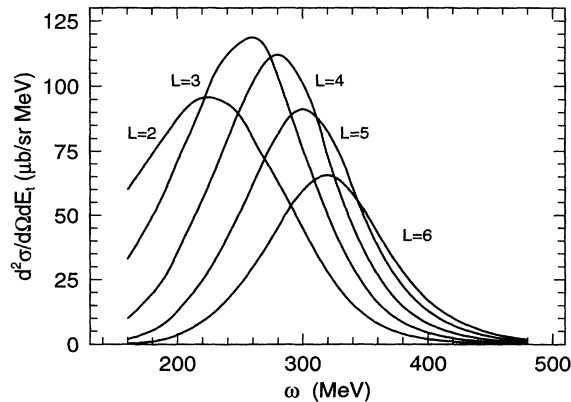


FIG. 7. Contribution of separate  $\Delta$ -hole multipoles.

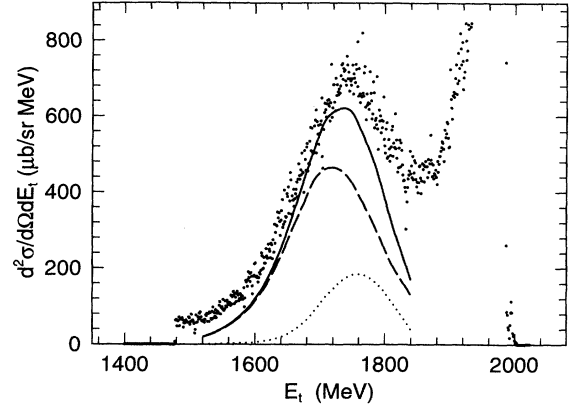


FIG. 8. Different contributions to the triton spectrum. Dashed line,  $\Delta$ -hole contribution. Dotted line, coherent pion production. Solid line, full spectrum.

#### D. Coherent pion production

Figure 8 shows the final triton spectrum together with separate contributions of the  $\Delta$ -hole excitations and the coherent pion production. The process of coherent pion production gives sizable contributions to the inclusive triton spectrum. The maximum of the cross section is at about 240 MeV excitation energy and it also contributes to the shift of the inclusive peak. The coherent pion production is absent in infinite nuclear matter, therefore one should expect a decrease of the relative yield of coherent pions for heavier nuclei.

The final curve in Fig. 8 still underestimates the height of the peak for 12% as well as the high-energy wing of the triton spectrum. One should remember, however, that we do not have free parameters in our calculation except  $g'_\Delta$ . The parameters of the elementary reaction amplitude and the wave functions of  ${}^3\text{He}$  and tritium were fixed in [13] from the analysis of the  ${}^1\text{H}(p, n)\Delta^{++}$  and  ${}^1\text{H}({}^3\text{He}, t)\Delta^{++}$  reactions. The fit of  $g'_\Delta$  from this only reaction is meaningless because it contributes to  $\Delta$  photo-production as well and they must be analyzed together. In addition, there are effects that were not included in this calculation and that can be important on the 10% level. First, at the high-energy wing of the triton spectrum the projectile  $\Delta$  excitation can contribute in inclusive reaction [10]. Second,  $d$ -wave admixture in  ${}^3\text{He}$  and triton wave functions was neglected in this calculation. As was shown in [20], the  $d$  wave together with exchange contributions change both longitudinal and transversal  $({}^3\text{He}, t)$  form factors. In the case of the reaction on nuclei, however, the form factors cannot be separated from distortion but inclusion of the  $d$  wave will influence the distortion factor changing the magnitude of the cross section.

#### VII. CONCLUSIONS

For the  $({}^3\text{He}, t)$  reaction in the  $\Delta$  region strong deviations from impulse approximations were found. The de-



viations come from the medium effects of renormalization of the pion propagator in the OPE mechanism of the elementary charge-exchange reaction. The medium effects change both the peak position and its height. Several effects, besides pion renormalization, contribute to the shift of the peak position including the  $\Delta$ -nucleus optical potential and coherent pion production. The possible enhancement in the  $\Delta$ -hole spectrum due to the  $\Delta$ -hole interaction is suppressed by incoherent  $\Delta$  decay. The effect of virtual pion propagation, however, manifests itself in the process of coherent pion production.

The finite size of a target nucleus produces together with the medium effects a large spreading of the observed peak. The absorption in initial and final states strongly

suppresses the lowest multipoles of the angular momentum transfer. The Glauber approach to the distortion in initial and final states gives a reasonable description of both the size of the medium effects and the magnitude of the cross section.

#### ACKNOWLEDGMENTS

During all stages of this work the discussions with Carl Gaarde and Thomas Sams were very stimulating and helpful. I would like to thank V. G. Zelevinsky and V. B. Telitsin for discussions of different aspects of the problem.

- 
- [1] C. Ellegaard *et al.*, Phys. Rev. Lett. **50**, 1745 (1983).
  - [2] V.G. Ableev *et al.*, JETP Lett. **40**, 763 (1984).
  - [3] D. Contardo *et al.*, Phys. Lett. **168B**, 331 (1986).
  - [4] C. Gaarde, Annu. Rev. Nucl. Part. Sci. **41**, 187 (1991).
  - [5] G. Chanfray and M. Ericson, Phys. Lett. **141B**, 163 (1984).
  - [6] V.F. Dmitriev and Toru Suzuki, Nucl. Phys. **A438**, 697 (1985).
  - [7] V.F. Dmitriev, Yad. Fiz. **46**, 770 (1987) [Sov. J. Nucl. Phys. **46**, 435 (1987)].
  - [8] S.W. Hong, F. Osterfeld, and T. Udagawa, Phys. Lett. B **245**, 1 (1990).
  - [9] J. Delorme and P.A.M. Guichon, Phys. Lett. B **263**, 157 (1991).
  - [10] E. Oset, E. Shiino, and H. Toki, Phys. Lett. B **224**, 249 (1989).
  - [11] H. Esbensen and T.-S.H. Lee, Phys. Rev. C **32**, 1966 (1985).
  - [12] V.F. Dmitriev, Phys. Lett. B **226**, 219 (1989).
  - [13] V.F. Dmitriev, O.P. Sushkov, and C. Gaarde, Nucl. Phys. **A459**, 503 (1986).
  - [14] E. Ferrari and F. Selleri, Phys. Rev. Lett. **7**, 387 (1961).
  - [15] G. Wolf, Phys. Rev. **182**, 1538 (1969).
  - [16] B.J. Vervest, Phys. Lett. **83B**, 161 (1979).
  - [17] A.B. Wiklund *et al.*, Phys. Rev. D **35**, 2670 (1987).
  - [18] A.B. Wiklund *et al.*, Phys. Rev. D **34**, 19 (1986).
  - [19] V.A. Karmanov *et al.*, Yad. Fiz. **18**, 1133 (1973) [Sov. J. Nucl. Phys. **18**, 583 (1973)].
  - [20] P. Desgrolard, J. Delorme, and C. Gignoux, Nucl. Phys. **A544**, 811 (1992).
  - [21] M.G. Olsson and E.T. Osypowsky, Nucl. Phys. **B101**, 136 (1975).
  - [22] M. Ericson and T.E.O. Ericson, Ann. Phys. (N.Y.) **36**, 323 (1966).
  - [23] Stephen J. Wallace, *Advances in Nuclear Physics* (Plenum, New York, 1981), Vol. 12.
  - [24] J. H. Koch, E. J. Moniz, and N. Ohtsuka, Ann. Phys. (N.Y.) **154**, 99 (1984).
  - [25] T.-S. H. Lee and K. Ohta, Phys. Rev. C **25**, 3043 (1982).